# Polymers, Phosphors, *and* Voltaics *for* Radioisotope Microbatteries

*Edited by*
Kenneth E. Bower
Yuri A. Barbanel'
Yuri G. Shreter
George W. Bohnert

CRC PRESS

# Polymers, Phosphors, *and* Voltaics *for* Radioisotope Microbatteries

# POLYMERS, PHOSPHORS, *and* VOLTAICS *for* RADIOISOTOPE MICROBATTERIES

*Edited by*
Kenneth E. Bower
Yuri A. Barbanel'
Yuri G. Shreter
George W. Bohnert


CRC PRESS

Boca Raton London New York Washington, D.C.

CRC Press
Taylor & Francis Group
6000 Broken Sound Parkway NW, Suite 300
Boca Raton, FL 33487-2742


Version Date: 20130919

International Standard Book Number-13: 978-1-4200-4139-2 (eBook - PDF)

# Preface

This book is a remarkable testament to the value of collaboration on technical problems with broad social implications. More than 30 scientists in Russia and the U.S. have worked together over the last several years on original research into radioisotope battery design optimization.

Progress on this topic has the potential to revolutionize microelectronics by enabling emerging microelectromechanical systems (MEMS) and nanotechnology. Power-matched supplies would last decades, even centuries. No power cords, rectifiers, or transformers will be needed for a new generation of microdevices — only safe, direct, long-life, stable, integrated electric power from the highest energy density source available.

A key feature of this book is discussion of the materials of construction for miniaturized radioisotope power supplies. Progress in nuclear battery technology depends on characterization of functionally radiation-stable components. Substantial progress has been made to solve problems of using integrated radioisotope batteries for micro- and nanoelectronics. Each author has provided an authoritative assessment and indicated where development is needed. The first chapter's treatment of ionizing radiation serves to remind us that *all* materials are ionized in the pressence of 5.5 MeV decay particles. We seek materials that are *functionally* stable — the components perform the engineered task even after ionization.

This book is intended for MEMS designers, electrical and nuclear engineers, material scientists in general and polymer and phosphor chemists in particular, voltaic fabricators, radioactive material policy makers, and other interested nuclear industry professionals.

Significant technological progress depends today on coordinated interdisciplinary research. A large group of scientists and technologists was organized around the shared applied goal of building a better radioisotope battery that can enable MEMS technology. We have had the privilege of serving as project leaders and now as editors on this project. We are grateful for the diversity of talent and specialties focused on this work. We have optimism for the future of the radioisotope microbattery as a commercially significant development and hope that our collaboration provides part of a multinational solution to nuclear fission waste disposition.

**Kenneth E. Bower,** Charleston, Illinois

**Yuri G. Shreter,** St. Petersburg, Russia

**Yuri A. Barbanel',** St. Petersburg, Russia

**George W. Bohnert,** Kansas City, Missouri

# The Editors

**Kenneth E. Bower** earned his Ph.D. in chemistry in 1991 from the University of Akron, Ohio. He was a postdoctoral fellow at Los Alamos National Laboratory in chelating polymer synthesis and a team leader for actinide analytical chemistry sample management. Dr. Bower is research director for TRACE Photonics Incorporated, which is integrating the radioisotope microbattery into sensors and MEMS. He resides in Charleston, Illinois, a few blocks from "The Castle" of Eastern Illinois University.

**Yuri G. Shreter** was born in 1944 in Petropavlovsk. He earned his B.Sc. in physics and engineering from the Odessa Technical University (1967) and his Ph.D. (1971) and Doctor of Science (1993) from A.F. Ioffe Physico-Technical Institute in St. Petersburg. Dr. Shreter became a visiting Gauss professor in Gottingen University, Germany (1987-88) and a visiting professor at Cologne University and at UMIST, Manchester, United Kingdom (1991-92). Dr. Shreter is currently a leading scientist at A.F. Ioffe Physico-Technical Institute and a professor at St. Petersburg State Technical University. His research interests include material science of wide-band-gap semiconductors and devices.

**Yuri A. Barbanel'** was born in 1935 in Leningrad (now St. Petersburg). He graduated from the chemistry department of Leningrad State University in 1958 and earned his Ph.D. in 1964 and his D.Sc. in 1991. Dr. Barbanel' is currently a leading scientist at V.G. Khlopin Radium Institute (St. Petersburg). His research interests include optical spectra (including radioluminescence), energy level structure of the lanthanide and actinide ions in crystals, and the absorption spectra of the actinides and lanthanides in molten salts.

**George W. Bohnert** is a senior staff engineer in the materials engineering and business development section of Honeywell Federal Manufacturing & Technologies, a prime contractor for the U.S. Department of Energy. He received his B.S. in chemical engineering from the University of Missouri at Columbia in 1976. He joined Honeywell in 1981. His research areas include polymer processing, precision cleaning, process waste minimization, and investigation of alternative energy technologies. Mr. Bohnert is a coinventor of three U.S. patents. He resides on a small farm near Harrisonville, Missouri with his lovely wife and two children.

# Acknowledgment

This collaboration was sponsored by Initiatives for Proliferation Prevention, U.S. Department of Energy, and administered by the U.S. Civilian Research and Development Foundation. TRACE Photonics Inc. was supported by U.S. Army, Picatinny Arsenal engineers, G. Robert Haugeto and Mike Kajor through the Small Business Innovated Research (SBIR) Program, and Sensor Technology Development Fund venture capital partners Robert Knollenberg and Betty Ohannessian.

# Contributors

**Gennady P. Akulov**
V.G. Khlopin Radium Institute
St. Petersburg, Russia

**Vyatcheslav M. Andreev**
Ioffe Physico-Technical Institute
St. Petersburg, Russia

**Laura Yu. Barbanel'**
St. Petersburg, Russia

**Yuri A. Barbanel'**
V.G. Khlopin Radium Institute
St. Petersburg, Russia

**Natalia I. Bochkareva**
Ioffe Physico-Technical Institute
St. Petersburg, Russia

**George W. Bohnert**
Honeywell FM&T
Kansas City, Missouri

**Carl C. Bower**
TRACE Photonics Inc.
St. Paul, Minnesota

**Kenneth E. Bower**
TRACE Photonics Inc.
Charleston, Illinois

**Victor A. Bykov**
V.G. Khlopin Radium Institute
St. Petersburg, Russia

**Tatyana A. Iourre**
Institute of Technology
St. Petersburg, Russia

**Yuri L. Kaminski**
V.G. Khlopin Radium Institute
St. Petersburg, Russia

**Alexander G. Kavetsky**
V.G. Khlopin Radium Institute
St. Petersburg, Russia

**Natalia V. Klimova**
Institute of Technology
St. Petersburg, Russia

**Piotr M. Konovalov**
V.G. Khlopin Radium Institute
St. Petersburg, Russia

**Sergei P. Meleshkov**
V.G. Khlopin Radium Institute
St. Petersburg, Russia

**Sergei N. Nekhoroshkov**
V.G. Khlopin Radium Institute
St. Petersburg, Russia

**Alexander A. Panferov**
V.G. Khlopin Radium Institute
St. Petersburg, Russia

**Yuri T. Rebane**
Ioffe Physico-Technical Institute
St. Petersburg, Russia

**Ludmila I. Rudaya**
Institute of Technology
St. Petersburg, Russia

**Andrew F. Rutkiewic**
TRACE Photonics Inc.
Albuquerque, New Mexico

**Yuri G. Shreter**
Ioffe Physico-Technical Institute
and St. Petersburg State Technical University
St. Petersburg, Russia

**Valentina B. Shuman**
Ioffe Physico-Technical Institute
St. Petersburg, Russia

**Maxim M. Sychov**
Institute of Technology
St. Petersburg, Russia

**Shahid M. Yousaf**
TRACE Photonics, Inc.
Charleston, Illinois

# Symbol Designations

| | |
|---|---|
| $A$ | Activity of radioactive substance |
| $A_{al}$ | Allowed activity of radioactive substance |
| $A_m$ | Specific activity of radioactive substance |
| $A_{mol}$ | Molar activity of radioactive substance |
| $A_S$ | Surface activity of radioactive substance |
| $A_v$ | Volumetric activity of radioactive substance |
| ARC | Antireflection coating in PV cells |
| $B$ | Brightness |
| $b(\lambda)$ | Relative spectral density of the radiant flux |
| $c$ | Speed of light |
| Ci | Curie unit, $3.7 \cdot 10^{10}$ disintegrations per second |
| $d$ | Substance density |
| $D_{abs}$ | Absorbed dose |
| $D_C$ | Cylinder diameter |
| $D_{el}$ | Electron dose |
| $D_g$ | Gelation dose |
| $D_L$ | Linear dimension (thickness, etc.) |
| $D_S$ | Sphere diameter |
| $d_S$ | Surface density of a substance |
| $E$ | Energy |
| $E_A$ | Process activation energy |
| $\mathrm{E_c}$ | Conduction band of semiconductor |
| $E_{av}$ | Average energy for creation of electron–hole pair |
| $\mathrm{E_F}$ | Fermi level in semiconductor |
| $E_g$ | Bandgap (energy) of semiconductor |
| $E_{lat}$ | Crystal lattice energy |
| $E_T$ | Energy of activation of nonradiative transition |
| $\mathrm{E_V}$ | Valence band in semiconductor |
| FF | Fill factor of current-voltage characteristics |
| $G$ | Radiation-chemical yield |
| $g_c$ | Gel fraction |
| $G_{el}$ | Electrical capacitance |
| $h$ | Planck's constant |
| $H_C$ | Cylinder height (length) |
| $I$ | Current (strength) |
| $I_{IC}$ | Ionization current |
| $\mathrm{I_O}$ | Saturation current in PV cell |
| $\mathrm{i_O}$ | Saturation current density in PV cell |
| $\mathrm{I_{PC}}$ | Photocurrent in PV cell |
| $I_{sc}$ | Short-circuit current |
| $\mathrm{i_{PC}}$ | Photocurrent density in PV cell |
| $k$ | Boltzmann's constant |
| $k_l$ | Light concentration coefficient |

| | |
|---|---|
| $K_m$ | Maximal luminous efficiency at the peak wavelength of 555 nm |
| $K_T$ | Temperature instability coefficient of energy efficiency |
| $L_L$ | Light output |
| L, $L_n$, $L_p$ | Diffusion length of carriers in semiconductor |
| $M$, $m$ | Mass |
| $M_A$ | Atomic mass |
| $M_M$ | Molecular mass |
| $N$ | Number of particles (atoms, electrons, etc.) |
| $N_A$ | Avogadro constant |
| $N_a$ | Acceptor concentration in semiconductor |
| $N_d$ | Donor concentration in semiconductor |
| $n_\beta$ | Beta particle flux |
| $n_i$ | Intrinsic carrier concentration in semiconductor |
| $\eta_o$ | Backscatter coefficient |
| $\eta$ | Efficiency of energy transfer, release, or conversion |
| $\eta_{CL}$ | Energy efficiency of cathodoluminescence |
| $\eta_d$ | Energy efficiency of direct conversion of energy |
| $\eta_{ind}$ | Energy efficiency of indirect conversion of energy |
| $\eta_{l\text{-}el}$ | Energy efficiency of conversion of light energy into electricity by a photovoltaic |
| $\eta_q$ | Quenching coefficient of luminescence |
| $\eta_{RL}$ | Energy efficiency of radioluminescence |
| $\eta_{st}$ | Stokes losses coefficient |
| $\eta_T$ | Thermalization coefficient |
| $\eta_\beta$ | Efficiency of conversion of beta particle energy into available surface beta flux |
| $\eta_{\beta\text{-}el}$ | Efficiency of conversion of beta particle energy into electricity by a betavoltaic |
| $\eta_{\beta\text{-}l}$ | Efficiency of conversion of beta particle energy to light |
| OPV | Organic photovoltaic cell |
| PV | Photovoltaic cell |
| $p$ | Pressure |
| P | Output electric power from PV cell |
| $P_D$ | Dose rate |
| $P_m$ | Maximal electrical power output of PV or betavoltaic cells |
| $P_{sp}$ | Specific (per 1 Ci) power of radiation of radioactive substance |
| $P_v$ | Specific (per unit volume) power |
| $P_\beta$ | Power of the beta particle flux |
| $Q$ | Carrier collection coefficient |
| $Q_{int}$ | Internal quantum yield of PV cells |
| $Q_{ext}$ | External quantum yield of PV cells |
| $q$ | Electron charge |
| $q_v$ | Frequency factor |
| $R$ | Resistance |
| $R_C$ | Cylinder radius |
| $R'_m$ | Maximal path length of particles in a substance |

| | |
|---|---|
| $R_o$ | Universal gas constant |
| $r$ | Distance in surface density units |
| $r_{op}$ | Primary electron backscattering coefficient |
| $S$ | Surface area |
| $s_c$ | Sol fraction |
| $s_o$ | Surface recombination velocity of carriers in semiconductor |
| $S_e$ | Energy radiosity |
| $S_e(\lambda)$ | Spectral density of energy radiosity |
| $S_V$ | Luminosity |
| $T$ | Temperature |
| $T'$ | Optical transmission |
| $T''$ | Optical loss |
| $T_{1/2}$ | Half-life |
| $t$, $\tau$ | Time |
| $U(\lambda)$ | Spectral luminous efficiency function of monochromatic photopic light |
| $V$ | Voltage |
| $V_C$ | Potential difference in $p$–$n$ junction of PV cell |
| $v$ | Volume |
| $V_{oc}$ | Open-circuit voltage |
| $W$ | Average energy of ion pair formation in gas |
| $w$ | Probability |
| $w_r$ | Radiative recombination probability |
| $w_T$ | Nonradiative recombination probability |
| $w(\varepsilon_\beta)$ | Spectral response of beta particles |
| $x$, $y$ | Chromaticity coordinates |
| $Z$ | Atom nucleus charge (atomic number) |
| $Z_{eff}$ | Efficient atomic number of substance |
| $\gamma$ | Share of backscattered electrons |
| $\delta$ | Spectral band half-width |
| $\varepsilon_{av}$ | Average kinetic energy of beta particles |
| $\varepsilon_d$ | Dielectric permittivity |
| $\varepsilon_{max}$ | Maximal kinetic energy of beta particles |
| $\varepsilon_\alpha$ | Kinetic energy of alpha particles |
| $\varepsilon_\beta$ | Kinetic energy of beta particles |
| $\theta$ | Azimuthal angle |
| $\lambda$ | Wavelength or radioactive decay constant |
| $\mu_L$, $\mu_m$ | Linear and mass absorption coefficient of beta particles |
| $\nu$ | Frequency |
| $\rho$ | Distance |
| $\Phi_e$, | Radiant flux in energy units |
| $\Phi_V$ | Light flux in photometric units |
| $\Phi_e(\lambda)$, $\Phi_e(\nu)$ | Spectral densities of radiant flux per unit wavelength and frequency ranges |
| $\phi$ | Polar angle |
| $\varphi(r)$ | Dose function of the point beta emitter (source) |

| | |
|---|---|
| $\Omega$ | Solid angle |
| IR | Infrared |
| LET | Linear energy transfer |
| LPE | Liquid phase epitaxy |
| MSA | Minimal significant activity of radioisotope |
| MOCVD | Metal organic chemical vapor deposition |
| NMR | Nuclear magnetic resonance |
| RLS | Radioluminescent light source (RLSs – sources) |
| RLS-T | Tritium-based radioluminescent light source (RLSs-T – sources) |
| RTL | Radiothermoluminescence |
| UV | Ultraviolet |
| $x$ | Mole fraction of component in (solid) solution |

# Contents

# CHAPTER 1

# Conversion of Radioactive Decay Energy to Electricity

**A.G. Kavetsky, S.P. Meleshkov, and M.M. Sychov**

## CONTENTS



0-8493-0915-8/01/$0.00+$1.50

## 1.1 INTERACTION OF IONIZING RADIATION WITH MATTER

### 1.1.1 Types and Energy of Radioactive Decay

Radioactivity is a property of atoms of unstable isotopes that enables them to spontaneously transform into atoms of other isotopes, with emission of charged particles and quanta of electromagnetic radiation. Natural radioactivity was discovered by Becquerel in 1896 in the study of uranium salts; this marked the beginning of comprehensive examination and use of the phenomenon. A very interesting application is the use of energy released in radioactive decay for generation of electrical energy.

Spontaneous radioactive decay involves transformations of an unstable atomic nucleus leading to changes in its charge ($Z$), mass ($M$), and energy state. Several types of radioactive decay differ in the type of emitted particles. The most common types are alpha decay, electronic and positronic beta decay, and K-electron capture. Other kinds of radioactive decay do not play a significant role in practical applications of radioactivity.

Energy released in radioactive decay transforms into the kinetic energy of the daughter nucleus and emitted particles. This released energy is equal to the difference between the rest energy of the parent nucleus and the rest energy of the daughter nucleus and emitted particles. Kinetic energy of radioactive decay products (radioactive decay energy) can be converted into electricity. All types of radioactive decay obey the universal law of radioactive decay.

#### *1.1.1.1 Radioactive Decay Law*[1]

Variation of the number of radioactive atoms $N$ in time $t$ is proportional to $\exp(-\lambda t)$, where $\lambda$ is the radioactive decay constant. This relationship follows from the assumption that the probability of decay of a nucleus of a given kind in a given period of time is constant. Indeed, d$N$ minus the number of atomic nuclei decaying in the period from $t$ to $t + \mathrm{d}t$ is proportional to the time period d$t$ and the number of nuclei $N$ remaining by the time $t$:

$$\mathrm{d}N = -\lambda N \,\mathrm{d}t \tag{1.1}$$

The term $\lambda$ in Equation 1.1 is the radioactive decay constant characterizing the probability of decay in unit time. Integration of Equation 1.1 with respect to time from 0 to $t$, assuming the number of atoms at $t = 0$ is equal to $N_o$, gives

$$N = N_o \cdot \exp(-\lambda t) \tag{1.2}$$

Equation 1.2 describes the statistical law of spontaneous radioactive decay of an isolated radionuclide. It is convenient to characterize the lifetime of a radioactive isotope by a period in which half of the initial number of its nuclei undergo decay. This period is termed the half-life, $T_{1/2}$.

$$T_{1/2} = \frac{\ln 2}{\lambda} \tag{1.3}$$

The most important characteristic of a radioactive substance is its activity, $A$. Activity is the number of nuclei of a given isotope decaying in unit time. As follows from Equation 1.1, $A$ is the product of the decay constant and the number of radioactive nuclei in the sample:

$$A = -\frac{dN}{dt} = \lambda N \tag{1.4}$$

In the International System of Units, the dimension of activity is decay per second, becquerel (Bq). Another widely used activity unit is curie (Ci), equal to $3.7 \times 10^{10}$ Bq.

Alpha decay is characteristic of natural and artificial radioactive isotopes with large atomic numbers.[1,2] For unstable atomic nuclei, it is accompanied by emission of alpha particles, i.e., double-ionized helium atoms. Alpha decay yields a daughter nucleus whose mass number is lower than that of the parent nucleus by four units and of the charge by two units. The alpha particles emitted in decay of a given nucleus can have the same energy or a set of discrete energies. When a radionuclide emits several groups of alpha particles with different discrete energies, the decay is accompanied by emission of gamma quanta of different discrete energies because the nuclei formed by alpha decay can occur in different energy states. Transitions of nuclei from the excited states to the ground state are accompanied by gamma emission, with the energy of the emitted quanta equal to the difference between the energies of the corresponding two groups of alpha particles (with correction for nucleus recoil energy).

The energy of alpha particles emitted in radioactive decay for the overwhelming majority of alpha-emitting nuclei ranges from 4 to 9 MeV, and the energy of the concomitant gamma quanta usually does not exceed 0.5 MeV. Alpha particles carry the major fraction of energy released in the decay. Only about 2% of the energy (for heavy radioactive nuclei) transforms into the kinetic recoil energy of the daughter nucleus.

Another type of radioactive decay is transformation of radioactive nuclei with preservation of their mass numbers and increase (electronic beta decay) or decrease (positronic beta decay, $K$-electron capture) of the charge of the nuclei formed.[1-3] The energy released in beta transformations of a radioactive nucleus ranges from 0.018 ($^{3}$H) to 16.4 MeV ($^{12}$N).

Electronic beta decay is characteristic of nuclei of both natural and artificial radioactive elements; it is accompanied by emission of an electron and an antineutrino, $\tilde{\nu}$. Owing to random distribution of decay energy between the two particles emitted in electronic decay, the energy spectrum of beta particles is continuous and covers the range from zero to the maximal energy of the beta particle. A typical example of electronic beta decay is the beta decay of tritium with a half-life equal to 12.34 years:

$$^{3}_{1}\mathrm{H} \xrightarrow{12.34\ \text{years}} {}^{3}_{2}\mathrm{He} + \beta^{-} + \tilde{\nu}$$

Positronic beta decay is characteristic only of artificial radionuclides and is accompanied by transformation of one of the protons in the nucleus into the neutron with emission of positron and neutrino. The energy spectrum of positrons is continuous, as is that of beta particles. After escape from the nucleus, the positron unites with an electron to form two gamma quanta (0.51 MeV each).

*K*-electron capture is electron capture by electronic shells of the radionuclide. This competes with positronic beta decay. Capture from the closest electronic shell (*K* shell) is most probable, although capture from other shells (*L*, *M*, etc.) is also possible. This process is followed by electronic transitions to fill the vacancy formed in the electronic shells. Electronic transitions between shells of the forming atoms are accompanied by emission of characteristic x-ray radiation. Transition of an electron from an external electronic shell to the electronic vacancy can also occur without emission of x-ray quantum but with emission of another electron from the external (more remote than the nucleus) electronic shell (an Auger electron). The kinetic energy of the Auger electron is equal to the difference between the binding energy of the captured electron and that of the emitted electron. An example of an isotope that decays by *K*-electron capture is $^{55}$Fe.

Electronic and positronic beta decay and K-electron capture (beta transformations), as well as alpha decay, can be accompanied by emission of gamma quanta of various discrete energies in cases when the daughter nucleus is formed in an excited state. Transition to the ground state is accompanied by emission of gamma quanta and can occur in several steps through intermediate excited levels. The energy of gamma quanta accompanying beta decay can reach 2.5 MeV.

### 1.1.2 Interaction of Ionizing Radiation with Matter

Ionizing radiation can interact with matter to give various effects, some of which offer a possibility of generating electrical energy. Ionizing radiation emitted in radioactive decay is a flux of charged particles or electromagnetic quanta. When passing through matter, ionizing radiation loses energy in elastic and nonelastic interactions with electrons and nuclei of atoms of the substance. In elastic scattering, the initial particles do not disappear, no new particles appear, and particles (e.g., nuclei) involved in the interaction do not change their internal energy. The total kinetic energy of particles participating in elastic interaction remains unchanged and is redistributed among these particles with changing of interacting particle motion directions. Nonelastic interaction is characterized by conversion (complete or partial) of the kinetic energy of the moving particle to other forms, e.g., to the excitation energy of atom or nucleus, radiation energy, and rest energy of newly formed particles.

In this section, the main concern is with the primary processes occurring in interaction of the ionizing radiation with matter. Secondary processes, such as luminescence, generation of electron–hole pairs, and radiolysis will be discussed in later sections of this book.

### 1.1.2.1 Interaction of Alpha Particles with Matter[1-3]

When passing through an exposed substance, alpha particles lose their energy in nonelastic and elastic scattering with electrons and elastic scattering with nuclei. The main mechanism of the energy loss by alpha particles is their nonelastic Coulombic interaction with substrate electrons, which causes either ionization or excitation of atoms of the substance (ionization stopping).

In each event of nonelastic scattering of alpha particle causing ionization of the atom, one or several electrons are knocked out. The part of knocked-out high-energy electrons whose energy exceeds the ionization potential of atoms (delta electrons) can cause secondary ionization. Their behavior and character of interaction with the matter are similar to those of high-energy electrons and beta particles. The alpha particle gradually exhausts its energy, mainly in ionization-stopping events, until its energy becomes comparable with the average energy of thermal motion of medium particles. Collisions of alpha particles with nuclei and deviations of alpha particles from the beam due to scattering on nuclei are rare and do not noticeably contribute to the energy loss because of the low ratio of the nucleus diameter to the atom diameter (ca. $10^{-4}$).

The very low probability of elastic scattering of alpha particles on nuclei causes their trajectory to be nearly straight. The path length $R'$, which is the distance traveled by the alpha particle in the substance, depends on its initial energy, $E_{0\alpha}$. Empirical tables and formulas of alpha particle path length in various substances are given in physical handbooks. For example, the path length of $^{226}$Ra alpha particles ($E_{0\alpha}$ = 4.78 MeV) is about 3.3 cm in air under normal conditions and about 33 μm in water.[2]

### 1.1.2.2 Interaction of Beta Radiation with Matter[1-5]

In interaction with matter, beta particles, delta electrons, and monoenergetic accelerated electrons consume and lose their kinetic energy in multiple elastic and nonelastic scattering events with atoms of the irradiated substance (ionization loss). Electrons with high kinetic energy can lose part of their energy by generating bremsstrahlung (radiation loss), which arises when an electron is decelerated in the Coulombic field of a nucleus. In each event of interaction of incident electron with matter, the change in its momentum is relatively large, which can result in significant deviations from the initial motion direction. As a result, the motion in a substance of electrons with kinetic energy less than 100 keV is chaotic and resembles diffusion rather than forward motion in the initial direction.

The total loss of electron kinetic energy as it passes through matter is a sum of ionization and radiation losses:

$$\left(-\frac{\mathrm{d}E}{\mathrm{d}x}\right)=\left(-\frac{\mathrm{d}E}{\mathrm{d}x}\right)_{ion}+\left(-\frac{\mathrm{d}E}{\mathrm{d}x}\right)_{rad} \tag{1.5}$$

For nonrelativistic electrons (when $v/c << 1$, where $v$ is the electron velocity and $c$ is the light velocity), the specific ionization loss of kinetic energy of the incident electrons can be described by

$$\left(-\frac{\mathrm{d}E}{\mathrm{d}x}\right)_{ion} = \frac{4\pi q^4 ZN}{m_{oe}v^2} \ln\frac{m_{oe}v^2}{2J} \tag{1.6}$$

where $q$ is the electron charge, $m_{oe}$ is the electron rest mass, $N$ is the number of atoms in 1 cm$^3$ of the substance, $Z$ is the atomic number of the substance element, and $J$ is the average ionization potential of the substance atoms. Since $N = N_A\, d/M_A$, where $d$ is the substance density, $N_A$ is the Avogadro constant, and $M_A$ is the atomic mass of the substance, the specific ionization loss of kinetic energy of nonrelativistic electrons apparently increases with increasing density and atomic number (charge of atom nucleus) of the irradiated substance. At the same time, the specific ionization loss decreases with increasing kinetic energy of nonrelativistic electrons $E$, equal to $m_{oe}\, v^2/2$. The specific ionization loss of beta particles emitted by radionuclides used in nuclear batteries can be calculated by Equation 1.6; for alpha particles, similar equations can be used.

In accordance with classical electrodynamics, a decelerated electron stopping in the Coulombic field of an atomic nucleus with charge $Z$ emits electromagnetic energy proportional to the acceleration squared. Since the Coulombic force is proportional to the product of charges of the interacting particles and acceleration is proportional to the force and inversely proportional to the particle mass, the energy emitted in the course of particle stopping is proportional to $(Z/M)^2$, where $M$ is the particle mass. This dependence explains why the probability of energy emission by alpha particle during its stopping is lower by a factor of ca. $10^7$ than in the case of the electron stopping. Bethe and Heitler found that the specific radiation loss of electron kinetic energy depends on the degree of shielding of nucleus with atomic electrons. The following relation was found valid for the examined ranges of electron kinetic energy:

$$\left(-\frac{\mathrm{d}E}{\mathrm{d}x}\right)_{\mathrm{rad}} \sim Z^2 N\, E \tag{1.7}$$

According to Relation 1.7, radiation loss of electron kinetic energy increases in proportion to the squared charge $Z$ of the nuclei of the irradiated substance, with the concentration of atoms $N$ (and hence with the substance density), and with the electron kinetic energy.

The relation between radiation and ionization loss of electron kinetic energy can be estimated as

$$\frac{\left(-\mathrm{d}E/dx\right)_{\mathrm{rad}}}{\left(-\mathrm{d}E/dx\right)_{ion}} \approx \frac{EZ}{800} \tag{1.8}$$

This equation shows that, for electrons with high kinetic energy (more than 0.5 MeV) in substances with high $Z$, the radiation loss is comparable to ionization loss. When determining the energy loss from relatively low kinetic energy electrons such as tritium beta particles, radiation loss is small compared to ionization loss. However, the amount of soft beta emitters can be estimated from the intensity of the bremsstrahlung, and health safety considerations should include the radiation loss, even from soft betas.

The true path length $R'$ of electrons in a substance is determined from the total energy loss:

$$R' = \int_0^{E_0} \frac{\mathrm{d}E}{\mathrm{d}E/\mathrm{d}x} \tag{1.9}$$

where $E_o$ is the initial electron energy. The true path length is the electron path length along a curvilinear trajectory. The projection of the true path length onto the initial direction of electron motion is termed the maximal path length, $R'_m$; this quantity can be determined experimentally. Beta particles of a given spectral distribution are commonly characterized by the maximal path length $R'_m$ (or by the maximal depth of penetration of beta particles into substance) related to beta particles of the maximal energy $\varepsilon_{max}$. For aluminum, $R'_m$ is calculated by the empirical equation

$$R'_m = 0.412\,\varepsilon_{max}^{\left(1.256-0.0954\cdot\ln\varepsilon_{max}\right)} \quad \text{for } 0.01 \le \varepsilon_{max} \le 3 \text{ MeV} \tag{1.10}$$

In Equation 1.10, $R'_m$ is expressed in grams per square centimeter and $\varepsilon_{max}$ in MeV. In materials different from aluminum, $R'_m$ can be calculated by the equation

$$R'_{m,x} = R'_{m,\mathrm{Al}} \frac{\left(Z/M_A\right)_{\mathrm{Al}}}{\left(Z/M_A\right)_x} \tag{1.11}$$

where $R'_{m,x}$, $R'_{m,\mathrm{Al}}$, $(Z/M_A)_x$, and $(Z/M_A)_{\mathrm{Al}}$ are the maximal path lengths and charge-to-mass ratios for element $x$ and aluminum, respectively.

For a continuous spectrum of beta particles with energy varying from practically zero to $\varepsilon_{max}$, dependence of the flux density of beta particles $n_\beta$ on the substance layer thickness $r$ is approximately exponential, where $n_\beta^{\circ}$ and $n_\beta$ are the flux densities of beta particles in the incident beam. $\mu_m$ is the mass coefficient of beta particle absorption in cm$^2$/g.

$$n_\beta = n_\beta^{\circ} \exp\left(-\mu_m \cdot r\right) \tag{1.12}$$

$$\mu_m = 15.5\,\varepsilon_{\max}^{-1.41} \tag{1.13}$$

### 1.1.2.3 Interaction of X-Ray and Gamma Radiation with Matter[1-5]

Interaction of hard electromagnetic quanta with matter is different from interaction of charged particles. First, hard electromagnetic quanta have zero rest mass and a velocity of light. Also, electromagnetic quanta have no charge and therefore are not subject to the action of long-range Coulombic forces. The probability of interaction of hard electromagnetic quanta with particles of a substance is considerably lower than for electrons and alpha particles, and the penetrating power of x-ray and gamma quanta is high.

Variation of gamma or x-ray quanta flux $\Phi$ passing through a substance of thickness $D_L$ is described by an exponential function.

$$\Phi\left(D_L\right) = \Phi_0 \exp\left(-\mu\ D_L\right) \tag{1.14}$$

where $\mu$ is the linear extinction coefficient of the gamma or x-ray quanta flux in the given substance, $cm^{-1}$.

Interaction of x-ray and gamma quanta with matter involves significant effects: the photoelectric effect (photoeffect), Compton (noncoherent) scattering, and formation of electron–positron pairs.

The photoeffect is nonelastic interaction of gamma quanta (electromagnetic radiation quanta) with bound atomic electrons, in which the whole energy of the primary quantum is transferred to an electron of one of the atom electronic shells. As a result, the electron that took up the energy (photoelectron) is emitted by the atom with a kinetic energy equal to the difference between the energy of the primary quantum and the binding energy of this electron in the atom.

Compton scattering is elastic interaction (collision) of the incident quantum (treated as a particle) with an atomic electron. A high-energy gamma quantum can be fully absorbed in the Coulombic field of an atom nucleus or electron to generate an electron–positron pair. The major contribution to absorption of electromagnetic radiation of energy equal to hundredth and tenth fractions of a megaelectron-volt is made by the photoeffect and Compton effect. Interaction of hard photon radiation with matter results in generation of high-energy electrons whose interaction with the matter will give rise to secondary effects.

### 1.1.2.4 Dose and Dose Rate[6]

The energy transferred to a substance by ionizing radiation is quantitatively characterized by the absorbed radiation dose. Absorbed radiation dose $D_{abs}$ is the ratio of the energy of charged particles or photons $E$, transferred by ionizing radiation in the volume element with mass $m$ to that mass:

$$D_{abs} = \frac{E}{m} \tag{1.15}$$

The dimensional unit of the absorbed dose is gray (Gy), equal to 1 J of absorbed energy per kilogram of a substance. The rad unit is often used, where 1 rad = 0.01 Gy. The absorbed dose rate $P_D$ is the dose absorbed in unit time:

$$P_D = \frac{D_{abs}}{t} \tag{1.16}$$

The dimension of absorbed dose rate is gray per second (Gy/s), equal to watt per kilogram (W/kg) (1 Gy/s = 1 W/kg).

## 1.2 BASIC PRINCIPLES OF CONVERSION OF RADIOACTIVE DECAY ENERGY TO ELECTRICITY

Radioactive decay energy can be converted into electricity through conversion of kinetic energy of particles formed in radioactive decay to thermal energy, with subsequent conversion of the thermal energy to electrical energy. Alternatively, incidental electromagnetic radiation can be converted to thermal and electrical energy. The second way involves generation of the electrical energy without a thermal cycle for nuclear batteries of various types (direct-charge, direct-conversion, or indirect-conversion nuclear batteries).

### 1.2.1 Thermoelectric Converters

Devices generating electrical energy from radioactive decay energy based on a thermal cycle use radionuclide heat sources (RHSs), which are hermetically sealed containers or ampules that hold the radionuclide-containing material (radioisotope fuel) as a safe thermal source. Particles and electromagnetic radiation generated by the radionuclide decay are absorbed in the radioisotope fuel and structural material of the RHS fuel ampule, and they give off heat. The thermal power $Q$ released at time $t$ can be estimated as

$$Q(t) = 3.7 \cdot 10^{10} \cdot A_o \cdot \varepsilon_{av} \cdot \exp(-\lambda t) \tag{1.17}$$

where $A_o$ is the radionuclide activity in Ci at time $t = 0$, $\lambda$ is the radioactive decay constant, and $\varepsilon_{av}$ is the average energy of particles and quanta released in a decay event.

The characteristics of some $^{238}PuO_2$-based RHSs developed in the V. G. Khlopin Radium Institute, St. Petersburg, Russia, are listed in Table 1.1.

Of the many methods for conversion of thermal energy to electricity, the most suitable for RHSs are the dynamic (using the Renkin liquid–metal cycle or the Brighton gas cycle), thermoionic, and thermoelectric methods.[8,9]

The dynamic method for conversion of thermal energy to electricity is based on generation of electrical energy with a turbogenerator. The generator is driven by a circulating fluid in a closed circuit, which is evaporated (Renkin cycle) or heated

**Table 1.1 Characteristics of some RHSs**

| RHS Designation | Thermal Power, W | Working Temperature, °C | Year of Development |
|---|---|---|---|
| Zemlya-1 | 22 | 400 | 1966 |
| Zhizn' | 300 | 920 | 1968 |
| Sloi | 2 | 400 | 1970 |
| RHS | 120 | 900 | 1971 |
| Vysota | 1000 | 950 | 1978 |
| Pochva | 20 | 200 | 1984 |
| RHS-238-3, 7, 12 | Series: 3, 7, 12 | 110 | 1986 |
| Gemma-OKR | Series: 0.08–0.30 | 160 | 1987 |
| RHS-238-0.22 | 0.22 | 180 | 1990 |

*Source*: Bartenev, S.A. et al., Radionuclides and articles thereof for science, technology, and medicine, in *V.G. Khlopin Radium Institute. On the 75th Anniversary*, Il'enko, E.I., Ed., St. Petersburg Institute of Nuclear Physics, 1997, 133 [Russian language].

(Brighton cycle) by a radionuclide fuel block.[8,9] The SNAP-1 unit developed in the 1950s in the U.S. utilized 3.5 MCi $^{144}$Ce ($A_m$ = 3183 Ci/g for 100% $^{144}$Ce, $T_{1/2}$ = 284 days) as the heat source, generated 500 W of electrical power at 115 V, and had a conversion efficiency of about 10%. The theoretical efficiency limit for dynamic energy conversion is 15% for electrical output greater than 1 kW.[9] However, dependence on many moving parts, necessity of using huge quantities of radioisotope fuel, and low conversion efficiency for electrical power less than 1 kW severely restricted possible applications.[8,9]

The thermoionic method for conversion of thermal energy to electricity is based on the thermoelectron emission phenomenon. When heated to a high temperature (up to 1700°C), a cathode emits electrons that pass through alkali metal (cesium) vapor to eliminate space charge and are collected on an anode kept at a considerably lower temperature (up to 700°C).[8] The theoretical efficiency of thermoionic devices is predicted to reach 20%, with short-circuit current density as high as 100 A/cm$^2$, 0.7 V between converter terminals at maximal power, and continuous operation for 20,000 hours.[8] The SNAP-13 radionuclide thermoionic generator containing the radioisotope $^{242}$Cm generated 12.5 W.[9] Energy conversion efficiency was not optimal because of inadequate heat insulation at very high working temperatures. At these temperatures, stringent requirements are imposed on the strength and corrosion resistance of the fuel capsule, and the presence of cesium vapor further constrains material choices for emitter, collector, and insulators.

Dynamic and thermoionic methods cannot compete with the practical thermoelectric method. In 1929, Ioffe[8] was the first to propose thermoelectric converters for generation of electrical energy. Development of radioisotope thermoelectric generators (RTGs) was initiated in the U.S. in the early 1950s.[7,9]

The thermoelectric method for conversion of thermal energy to electricity is based on the thermoelectromotive force arising from a temperature gradient between two branches of an electric circuit composed of different conductors or semiconductors. Although designs of working RTGs are diverse,[8-10] their principal scheme is similar. Figure 1.1 shows the principal scheme of an RTG with external electrical

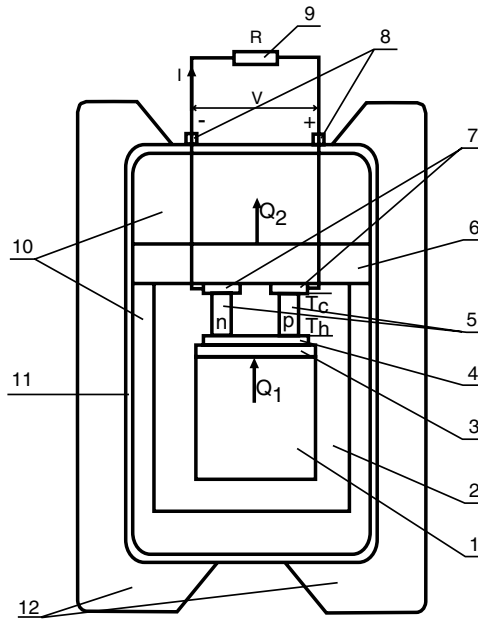


**Figure 1.1** Principal scheme of RITEG: (1) RHS, (2) thermal insulation, (3) hot heat conductor, (4) commutating plate of the hot junctions, (5) semiconductor branches with different types of conductivity, (6) cold heat conductor, (7) commutating plates of cold junctions, (8) power points, (9) external electric resistance, (10) biological shield, (11) casing, and (12) cooling ribs. Designations: $T_h$, $T_c$ are the temperatures of hot and cold junctions, respectively; $Q_1$, $Q_2$ are heat power emitting by RHS and dissipated heat power, respectively.

load. For optimal utilization of thermal power, several RHSs are arranged in a fuel container in the center of the RTG. The hot junctions of the thermocouples commutated in blocks are in thermal contact with the side or butt surfaces of the fuel container.

The cold junctions of the thermocouples are cooled by heat removal through the heat conductor, casing, and cooling ribs of the RTG, which also includes devices for thermal and electric control (not shown in Figure 1.1). These devices are intended for stabilization of the electric parameters of the RTG at a preset working level, since the generated thermal and electric power decrease in the course of operation according to radioactive decay law. To reduce the dose rate of ionizing radiation to a safe level, RTGs are equipped with a biological shield; its material and design depend on the kind and activity of radioisotope fuel.

RTGs are used in various autonomous devices. Among such devices are electric cardiostimulators, autonomous power sources for optical and radio beacons, meteorological stations, deep-sea buoys, and spacecraft electronics. The main characteristics of RTGs are listed in Table 1.2. The electric power generated by RTGs ranges from $10^{-3}$ to $10^2$ W; the efficiency of energy conversion is up to 6%.[8-10] RTGs often utilize the radioisotope $^{90}Sr$ because of its relatively low cost and availability[11]; $^{238}PuO_2$ is preferred in spacecraft RTGs and for use in electric cardiostimulators.

**Table 1.2 Characterization of RITEGs**

| Designation, Country | Power, W | | Voltage, V | Efficiency, % | Radionuclide | Fuel Loading, Ci (g) | Service Life, Years | Mass, kg | Ref. |
|---|---|---|---|---|---|---|---|---|---|
| | Thermal | Electrical | | | | | | | |
| SNAP-3B7, U.S. | 52 | 2.7 | 3.5 | 5.2 | $^{238}$Pu | 1,600 | 5 | 2.1 | 9, 10 |
| SNAP-7B, U.S. | 1440 | 68 | 12 | 4.7 | $^{90}$Sr | 225,000 | 10 | 2090 | 9 |
| SNAP-7C, U.S. | 256 | 11.6 | 5 | 4.5 | $^{90}$Sr | 40,000 | 10 | 850 | 9 |
| SNAP-11, U.S. | 396 | 19 | 3 | 4.8 | $^{242}$Cm | (6.2) | 0.5 | 7.55 (without protection) | 9 |
| SNAP-17, U.S. | — | 30 | — | — | $^{90}$Sr | — | 5–10 | 11.4 | 9 |
| SNAP-27, U.S. | — | 63 | | | $^{238}$Pu | — | 1 | 14 | 9 |
| RTG-3, U.S. | — | 1 | — | — | $^{238}$Pu | — | 20 | 4.4 | 9 |
| RIPPLE-1, GB | — | 0.075 | — | 1.71 | $^{90}$Sr | — | — | 600 | 9 |
| Beta-3, USSR | 265 | 12 | 12 | 4.5 | $^{90}$Sr | 40,000 | 10 | 250 | 8 |
| Beta-h, USSR | 208 | 10 | 6 | 4.8 | $^{90}$Sr | 31,000 | 10 | 156 | 8 |
| G-90-60/40, USSR | 1650 | 60 | 40 | 3.6 | $^{90}$Sr | 250,000 | 10 | 1200 | 8 |
| Ritm, USSR | 0.2 | $10^{-3}$ | 1 | 0.5 | $^{238}$Pu | — | 10 | 0.050 | 8 |

The major factor restricting application of RTGs is that they require large amounts of radiotoxic nuclides such as $^{90}$Sr and $^{238}$Pu. Small quantities of the isotopes do not generate sufficient thermal gradients. On the other hand, the use of pure beta emitters with energy less than 200 to 300 keV is relatively safe. Even large amounts of radionuclides such as tritium and $^{63}$Ni do not require heavy biological shields. Although the power released in beta decay of these radionuclides is insufficient for their use in RTGs, their beta radiation can be used for energy generation in nuclear batteries.

### 1.2.2 Direct-Charge Nuclear Batteries

The operational principle of direct-charge nuclear batteries is based on the fact that the voltage across the battery electrodes (emitter and collector) is provided by direct collection of charged particles on one of the electrodes (collector). Direct-charge nuclear batteries allow high voltages (up to hundreds of kilovolts) to be obtained at small currents (nanoamperes) determined by the rate of the radionuclide decay. The electricity is discharged by close of the circuit through a working load.

In the simplest case, such a nuclear battery consists of two concentric, coaxial, or parallel electrode surfaces insulated from each other and separated by an evacuated space or a space filled with a dielectric.[8,9] A radioactive substance emitting charged particles can be applied as a thin layer on the surface of one of the electrodes (emitter)[12,13] or, if it is gaseous (tritium, $^{85}$Kr), placed in the sealed interelectrode space of the battery.[9,14] Some of the charged particles formed by the radioactive decay and ejected toward the collector are collected on its surface. The charge transfer to the collector at the open electric circuit can continue (in the ideal case) until voltage across the electrodes reaches the value close to the maximal kinetic energy of the charged particles emitted by the radioactive substance.

To reach the collector, the charged particles must overcome the electrostatic field of like charge already built up. Very high voltage is limited by the internal resistance of the nuclear battery components, even in the open-circuit state. Charge is lost by leakage through the insulator surfaces (in the case of evacuated interelectrode space) or through the surface of the dielectric separating the electrodes. Therefore, the maximal voltage $V_{oc}$ generated at open circuit depends on the energy of the charged particles emitted by the radioactive substance and the nature of the dielectric separating the electrodes. $V_{oc}$ can be calculated by Equation 1.18[9]:

$$V_{oc} = R_i I \tag{1.18}$$

where $R_i$ is the internal resistance of the battery and $I$ is the charge current due to the radionuclide decay.

When the battery electrodes are closed through a loading resistance $R_e$, the current $I$ passes and the voltage $V$ decreases to the value given by Equation 1.19.[9]

$$V = R_{sum} I = \frac{R_e R_i I}{R_e + R_i} \tag{1.19}$$

In this case, the power $P$ of the nuclear battery whose emitter gives off charged particles in an angle of $2\pi$ can be estimated by Equation 1.20[8]:

$$P = I \cdot V = \eta \, D_L \, P_v \, S \tag{1.20}$$

where $I$ and $V$ are the working current and voltage, respectively, $\eta$ is the efficiency of the nuclear battery, $D_L$ is the radionuclide layer quantity, $P_v$ is the specific (per unit volume) power of the radionuclide, and $S$ is the area of the emitting surface of the emitter.

Equation 1.20 shows that, to increase the power of direct-charge nuclear batteries, it is necessary to increase the working surface area of the electrodes and battery efficiency. This can be done by choosing the radionuclide layer thickness and the emitter thickness appropriately, so absorption of charged particles in these layers is minimal and emission of charged particles from the emitter surface occurs in a solid angle of $4\pi$ at maximal current densities.

The first nuclear battery operating according to this principle was suggested by Moseley in 1913.[15] For the emitter, he used a thin-walled spherical quartz ampule filled with radium. The ampule walls retained alpha particles but transmitted beta particles. This ampule was concentrically fixed with a thin quartz rod inside a sphere, with the silver-plated inner surface serving as collector of beta particles. After evacuation of the space between the sphere surfaces, an open-circuit voltage of 150 kV was obtained corresponding to electric breakdown on the insulator surface. The current at electrode closure was $10^{-11}$ A.

In a vacuum nuclear battery based on $^{90}$Sr and $^{90}$Y and developed by Linder,[12] the emitter of beta particles was a thin-walled (about 20 μm) complex-shaped tubular structure with spherical ends. The inner surface of this structure was coated with a layer of the radioisotope. The output open-circuit voltage of this battery reached 365 kV and the short-circuit current was about 1 nA. The efficiency of Linder beta radiation utilization (relative to the total amount of beta particles formed in radioactive decay) was about 75%, while the efficiency of Moseley's battery was 8%.[8]

As a practical example of a nuclear battery utilizing alpha emitters for generating high voltage across the electrodes, a design resembling a triode has been constructed and characterized.[16] The design includes a cylindrical emitter coated with $^{210}$Po on its external surface, coaxially fixed inside a cylinder of a larger diameter (collector) and separated from the collector by a control grid. A negative potential of several hundred volts, fed to the control grid, suppresses the current of secondary electrons arising from interaction of alpha particles emitted by $^{210}$Po with the emitter matter. The open-circuit voltage across the electrodes of this nuclear battery was 50 kV at a control grid voltage of –800 V and residual pressure in the interelectrode space of about 0.1 Pa.[8] The characteristics of other direct-charge batteries are listed in Table 1.3.[8,9]

Direct-charge nuclear batteries produce a high voltage (tens and hundreds of kV) and operate in the pulse mode at the engineered breakdown target; the electric power generated by them ranges from micro- to milliwatt, since the current is proportional to the flux of charged particles and does not exceed fractions of milliampere. The

**Table 1.3 Characteristics of Some Direct-Charge Nuclear Batteries**

| Radionuclide | Activity, Ci | Interelectrode Space | emf, V | $I_{sc}$, A | Mass, kg | Service Life, Years |
|---|---|---|---|---|---|---|
| $^{3}H$ | 0.2 | Vacuum | 1200 | $5 \cdot 10^{-10}$ | 0.02 | Weeks |
| $^{85}Kr$ | 0.04 | Polystyrene | 3000 | $10^{-10}$ | 0.03 | 5–10 |
| $^{85}Kr$ | 0.3 | Polystyrene | 5000 | $10^{-9}$ | 0.03 | 5–10 |
| $^{85}Sr$ | 0.02 | Polystyrene | 2000 | $5 \cdot 10^{-11}$ | 0.15 | >5 |

*Source*: Corliss, W.R. and Harvey, D.G., *Radioisotopic Power Generation*, Prentice-Hall, Inc., Englewood Cliffs, NJ, 1964.

extremely high efficiency of this approach suggests the value of designing the electronic load around this pulse mode capacitor.

### 1.2.3 Direct-Conversion Nuclear Batteries

Research on direct conversion of radioisotope decay energy followed several lines,[9] including nuclear batteries with contact voltage electrodes. In such batteries, any kind of radiation (alpha, beta, or gamma) causes volumetric ionization of the gas filling the space between two metal electrodes that have different work functions. The electrode contact potential difference creates an electric field carrying electrons and positively charged ions in opposite directions. Upon switching in an external load, an electric current passes in the circuit, depending on the kind and intensity of ionizing radiation as well as on the nature and pressure of the interelectrode gas, electrode material, etc. These nuclear batteries using 10 mCi $^{90}Sr$ created a voltage of about 1 V with short-circuit current of $4 \cdot 10^{-10}$ A.[9] However, the energy conversion efficiency for such batteries was low (0.5%), mainly because of high average energy of ion pair formation in the gas (about 30 eV).

Much greater promise is offered by beta flux irradiation of semiconductor elements of different conductivity types (*p–n* or *p–i–n* junctions). This is based on separation of the electron–hole pairs originating on exposure of the semiconductor materials by an electric field created by *p* and *n* layers of the *p–n* or *p–i–n* junctions. As a result, the *n*-region charges negatively and the *p*-region charges positively. As every beta particle creates in a semiconductor material up to several tens of thousands of electron–hole pairs, *p–n* junction–based devices convert a small number of high-energy beta particles to a much greater current of low-energy electrons. However, not all electron–hole pairs created by beta radiation are involved in the current generation in the external circuit. The factors responsible for electron–hole pair loss are analyzed in Section 7.2 in Chapter 7.

The initial stage in conversion of the ionizing radiation energy (subsequent discussion will concern only beta radiation) to electrical energy consists in the outlet of the beta flux from the radionuclide-containing substance. The betas of the radionuclides typically employed in nuclear batteries have a fairly low energy whose portion will be lost by absorption in a carrier substance. Where the efficiency of conversion of the total beta energy to a beta flux energy at the source surface is $\eta_\beta$ (the remainder being self absorbed) and the efficiency of conversion of the beta flux

energy to electrical energy is $\eta_{\beta\text{-}el}$, the efficiency of the direct energy conversion is equal to the product

$$\eta_d = \eta_\beta \cdot \eta_{\beta-el} \tag{1.21}$$

The efficiency of the current generation in the external circuit $\eta_{\beta\text{-}el}$ can be defined as the ratio of the electrical power generated under optimum external load to the beta flux power absorbed in the semiconductor. (This definition is not the same as the ratio of electrical power to the activity of the source, which is included in the term $\eta_\beta$.) Owing to the loss of electron–hole pairs, the $\eta_{\beta\text{-}el}$ parameter is much less than unity. The dependence of $\eta_{\beta\text{-}el}$ on the band gap energy of the semiconductor has been theoretically calculated.[17] This calculation shows that for semiconductors with the band gap energy $E_g$ of 1.9 eV (AlGaAs), $\eta_{\beta\text{-}el}$ can reach 20 to 22%, and for those with 1.1 eV (Si), $\eta_{\beta\text{-}el}$ can reach 13 to 14%. At low excitation levels characteristic of a semiconductor exposed to tritium beta particles, the energy conversion efficiency $\eta_{\beta\text{-}el}$ is equal to 15% and 7 to 8% for AlGaAs- and Si-based semiconductors, respectively. The practically achievable $\eta_{\beta\text{-}el}$ values for selected betavoltaics are given in Table 1.4.

A typical scheme of a device generating electrical energy via exposure of a semiconductor converter to ionizing radiation is shown in Figure 1.2. It includes a source of radioactive radiation and a converter. Different designs utilize diverse sources of ionizing radiation and betavoltaic converters. The performance characteristics of selected devices are presented in Table 1.4. These refer, for the most part, to prototype models of direct-conversion betavoltaics. Commercial "beta cell" (McDonnell- Douglas) batteries are included in Table 1.4. The beta cell design is shown in Figure 1.3a, and its current-voltage characteristic is given in Figure 1.3b.

Table 1.4 also presents the efficiencies of conversion of energy of the beta flux from gaseous tritium to electrical energy by betavoltaics such as GaP, $Al_{0.1}Ga_{0.9}As$, and amorphous silicon (items 5, 6, and 7). The same table presents the characteristics of two models of direct-conversion nuclear batteries with solid-state tritium-based beta sources: those with titanium-tritide beta source (item 9) and with tritium incorporated into the *i*-layer of the *n–i–p* silicon converter (item 8). Table 1.4 shows that the greatest efficiency is exhibited by wide-band gap betavoltaics based on GaP and AlGaAs ($\eta_{\beta\text{-}el}$ of 5 to 6%).

Thus, nuclear batteries employing semiconductors converting decay energy to electrical energy via *p–n* junction significantly surpass in conversion efficiency those employing the contact voltage. Their conversion efficiency can reach several percent. For tritium-based nuclear battery models, the current density generated by the betavoltaic can reach 1 $\mu A/cm^2$, and for the open-circuit voltage of serially connected betavoltaics, it can reach several volts.

### 1.2.4 Indirect-Conversion Nuclear Batteries

Besides research into direct conversion of the energy of ionizing radiation into electrical energy, research into indirect energy conversion has also been performed

**Table 1.4 Characteristics of Direct-Conversion Betavoltaics**

| | Battery Units | | Battery Parameters | | | | | |
|---|---|---|---|---|---|---|---|---|
| No. | Radiation Source | Converter | $P_m$, μW $\left(\frac{dP_m}{dS}, \text{W/cm}^2\right)$ | $V_{oc}$, V | $I_{sc}$, μA ($i_{sc}$, μA/cm²) | Diameter × height, mm × mm | $\eta_d$, % ($\eta_{\beta\text{-}el}$, %) | Ref. |
| 1 | $^{90}$Sr - $^{90}$Y, $A$ = 50 mCi | Silicon, *n–p* | 0.8 | — | — | — | 0.94 | 8 |
| 2 | $^{147}$Pm, $A_m$ = 680 Ci/g | Silicon, *n–p*, junction depth 3 μm | — | — | (10) | — | (1.5) | 8 |
| 3 | $^{147}$Pm ($Pm_2O_3$) | Silicon *n–p* (package of converters) | 43 | 1.79 | 44 | 1.2 × 0.78 | 1.04 | 8 |
| 4 | $^{147}$Pm ($Pm_2O_3$) | Silicon *n–p* (package of converters) | 212 | 4.75 | 77 | 1.32 × 1.57 | 0.84 | 8 |
| 5 | Tritium, gas, $p$ = 1.03 MPa, $D_L$ = 2 cm | GaP | (0.68) | 1.05 | (1) | — | (6) | 18 |
| 6 | Tritium, gas, $p$ = 0.206 MPa | $Al_{0.1}Ga_{0.9}As$, Converter at the center of a hemisphere with $D_S$ = 2 cN | (0.4) | 0.5 | (1) | — | (5) | 19 |
| 7 | Tritium, gas | Amorphous silicon, *n–i–p* | 0.129 | 0.44 | 0.58 | — | (1.2) | 20 |
| 8 | Tritium, in Si-$^3$H, 10 at.% of tritium ($5 \cdot 10^{21}$ at/cm³), at $D_L$ = 1 μm, $A_S$ = 0.024 Ci/cm² | Amorphous silicon, *n–i–p*, tritium in a composition of the *i*-layer. | ($6 \cdot 10^{-5}$) | 0.089 | ($9 \cdot 10^{-4}$) | — | 0.007 | 21 |
| 9 | Tritium, $Ti^3H_2$, $A_S$ = 0.22 Ci/cm² | $Al_{0.25}Ga_{0.75}As$ | (0.015–0.027) | 0.6 | (0.040–0.058) | — | (3–5) | 19 |

*Note*: Designations: $P_m$ is the electrical power released under optimal load; $V_{oc}$ is the open-circuit voltage; $I_{sc}$ is the short-circuit current; $i_{sc}$ is the short-circuit current density; $\eta_{\beta\text{-}el}$ is the efficiency of conversion of the beta particle energy to electrical energy by the betavoltaic; $\eta_d$ is the direct conversion efficiency.

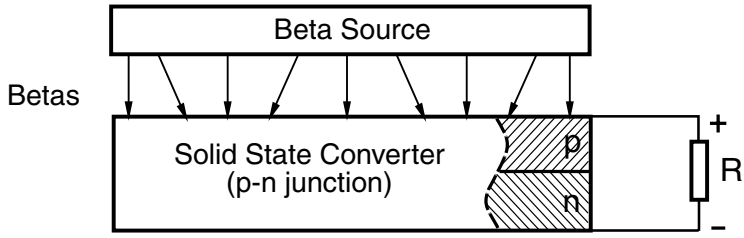


**Figure 1.2** Scheme of direct-conversion betavoltaic.

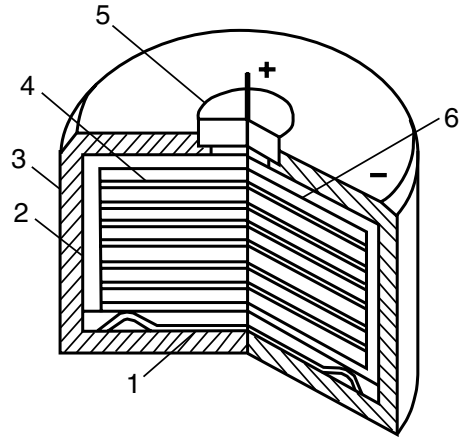


**Figure 1.3a** Betacel battery design: 1) spring; 2) insulating capsule; 3) case; 4) radiation source; 5) sealed contact; 6) silicon converter. (From Kodyukov, V.M. et al., *Radioisotope Sources of Electrical Energy*, Fradkin, G.M., Ed., Atomizdat, Moscow, 1978 [in Russian].)

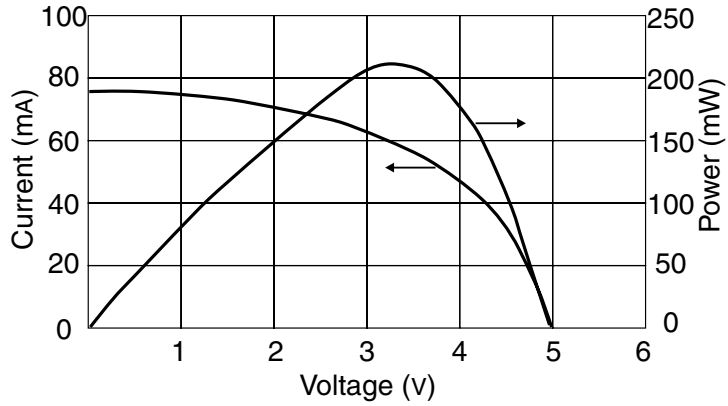


**Figure 1.3b** Current-voltage characteristic of betacel battery. (From Kodyukov, V.M. et al., *Radioisotope Sources of Electrical Energy*, Fradkin, G.M., Ed., Atomizdat, Moscow, 1978 [in Russian].)

since the 1950s. This method consists of conversion by radioluminescent materials of the energy released in the decay to energy of electromagnetic (light) radiation to be further converted to electrical energy by a photovoltaic. This is a two-stage conversion: radioactive radiation → light → electrical energy. This method may appear less efficient than the one-stage direct conversion: radioactive radiation → electrical energy. However, it has advantages in reduced radiation influence and in radiation protection of the sensitive photovoltaic element.

In both schemes, the initial stage of the energy conversion consists in the outlet of the beta flux from the radionuclide-containing carrier substance to its surface with conversion efficiency $\eta_\beta$. Conversion efficiency of beta particle energy to light energy is defined as $\eta_{\beta\text{-}l}$, and the efficiency of conversion of the light energy to electrical energy by a photovoltaic is defined as $\eta_{l\text{-}el}$. Hence, the indirect energy conversion efficiency $\eta_{ind}$ can be defined by:

$$\eta_{ind} = \eta_\beta \cdot \eta_{\beta-l} \cdot \eta_{l-el} \tag{1.22}$$

With appropriately chosen beta source designs, fairly high $\eta_\beta$ values can be achieved. For example, in certain modifications of tritium gas–filled radioluminescent light sources, $\eta_\beta$ is 0.84 (see Section 2.2.4.3 in Chapter 2). The efficiency of conversion of radioactive radiation to light by a luminescent material $\eta_{\beta\text{-}l}$ can reach 0.25 (see Section 3.1.1.1 in Chapter 3) and that of conversion of light energy to electrical energy on illumination of semiconductor converters to radioluminescent light sources can reach up to 0.35 (see Chapter 7). Hence, the conversion efficiency of indirect conversion $\eta_{ind}$ can attain 0.07. At the same time, Table 1.4 shows that, for direct-conversion breadboard batteries, $\eta_{\beta\text{-}el}$ does not exceed 0.06 and $\eta_d$ slightly exceeds 0.01. This suggests that optimization development for indirect conversion schemes is justified. Constructed prototypes of indirect conversion batteries are comparable in conversion efficiency to models of direct-conversion batteries.

Conceptual designs of betavoltaic batteries differ from each other in the type of the radioluminescent light source, radionuclide, and photovoltaic employed. The radionuclides most frequently used in such batteries are $^{147}$Pm and $^{3}$H. Early designs of the batteries utilized silicon, selenium, and cadmium sulfide–based photoelectric cells. Recently, photoelectric cells based on $A^3B^5$ compounds have been preferentially used.

The radioluminescent light source can be represented by:

- A mixture of powdered radionuclide-containing substance and a luminescent material[22]
- A powdered phosphor with a radionuclide incorporated in its crystal lattice[8]
- A mixture of gaseous radionuclides ($^{3}H_2$ or $^{85}$Kr) with inert gases (Ar, Kr, Xe) or inert gas–mercury vapor mixtures[22,23]
- Dusty solid particles containing alpha- or beta-emitting radionuclide, homogeneously dispersed in an inert gas (Xe); aerosols[11]
- A hermetic glass capsule of any shape whose inner surface is coated with a phosphor and whose cavity is filled with gaseous tritium[22,24-27]

- A panel comprising empty microspheres, filled with phosphor particles and gaseous tritium at elevated pressure[28]
- An aerogel–phosphor composition saturated with tritium[29]
- Other compositions, e.g., a mixture of an organic tritium–containing compound with an organic luminescent material (see section 2.3.6 in Chapter 2)

Electrical energy generation efficiency for any design of indirect conversion battery depends on how well matched the maxima of the spectral response curve of the semiconductor converter (photovoltaic) is to the emission maxima of the luminescent material.[8,11]

Selected schemes of indirect-conversion betavoltaic batteries are shown in Figures 1.4a to 1.4d. Table 1.5 presents characteristics of the betavoltaic batteries employing various light sources and photovoltaic converters, including activity of the radionuclide $A$, maximal electrical power $P_m$, volume of the battery $v$, specific (per unit activity) electrical power $Q$, and energy conversion efficiency $\eta_{ind}$. The parameter $Q$ characterizes the efficiency of the use of the radionuclide activity and is defined as the $P_m$-to-$A$ ratio. It is related to the energy conversion efficiency as

$$Q = P_{sp}\eta_{ind} \tag{1.23}$$

where $P_{sp}$ is the specific power released in the decay of 1 Ci of the radionuclide (data in Table 1.5 are initial values of the parameters of interest; the size of the battery is given without structural and enclosure units).

The $^{147}$Pm-based betavoltaic battery whose configuration is shown in Table 1.5 (item 1) was manufactured in the late 1950s[8] as the Elgin–Kidde atomic battery. It was characterized by a fairly high promethium-147 quantity and a service life of only 3 years. Thus, it had limited application.

The parameters of the batteries with a gas–dust mixture of the radioisotope-containing substance and a noble gas were calculated theoretically and presented in items 2 to 7 in Table 1.5. In this battery design, the decay energy is utilized efficiently. However, realization of such a device requires solving a number of problems. The first is to create a homogeneous stable gas–dust mixture and maintain it in this condition for a fairly long time (10+ years). The second problem is to create a wide-band-gap photovoltaic to convert vacuum UV radiation energy to electrical energy with high (up to 50%) efficiency. Notably, absorption of ionizing radiation by xenon causes radioluminescence with $\lambda_{max}$ = 172 nm. Such a converter can be based on doped diamond or aluminum nitride.[11] According to Baranov et al.,[11] prerequisites to finding a solution to these problems and creating this nuclear battery design exist.

The performance characteristics (radionuclide activity $A$, maximal electrical power $P_m$, and volume $v$) of the batteries with an aerogel–phosphor composition as the light source (items 8 and 9 in Table 1.5) were also calculated theoretically.[30] Such light sources with energy radiosity of 23 μW/cm$^2$ exhibit very unstable performance characteristics, owing to the high specific content of tritium.[30] Their radiosity decreases tenfold within 250 days.[29] The aerogel–phosphor composition,

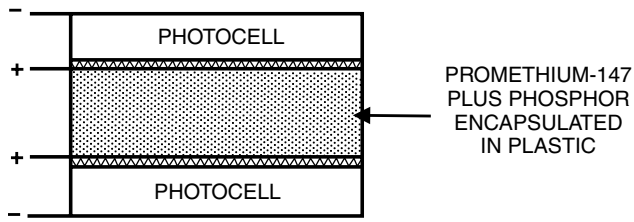


**Figure 1.4a** Phosphor + promethium oxide mixture–filled light source–based battery. (From Walko, R.J. et al., Electronic and photonic power applications, in *Radioluminescent Lighting Technology. Technology Transfer Conference Proceedings*, U.S. DOE, Annapolis, MD, 1990, 13-1.)

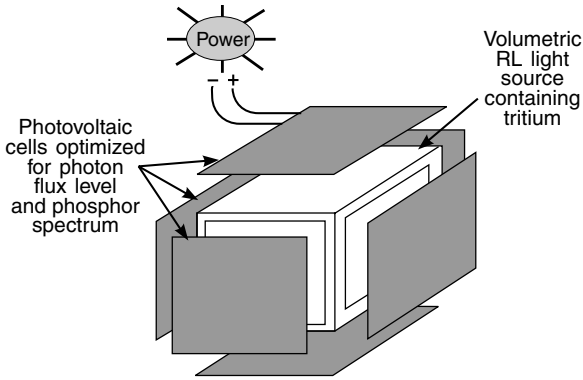


**Figure 1.4b** Aerogel–phosphor composition–filled (volumetric) light source–based battery. (From Walko, R.J. et al., Electronic and photonic power applications, in *Radioluminescent Lighting Technology. Technology Transfer Conference Proceedings*, U.S. DOE, Annapolis, MD, 1990, 13-1.)

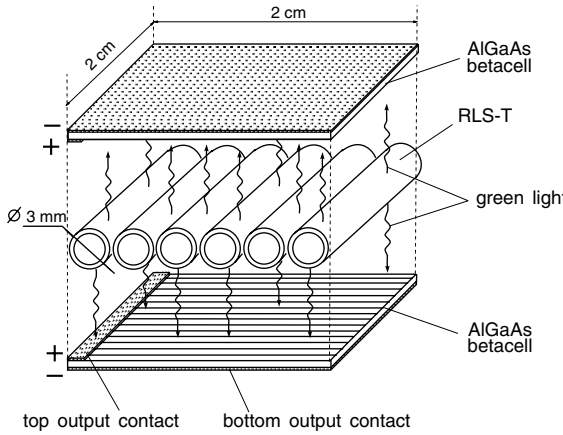


**Figure 1.4c** Tritium gas–filled light source–based battery.

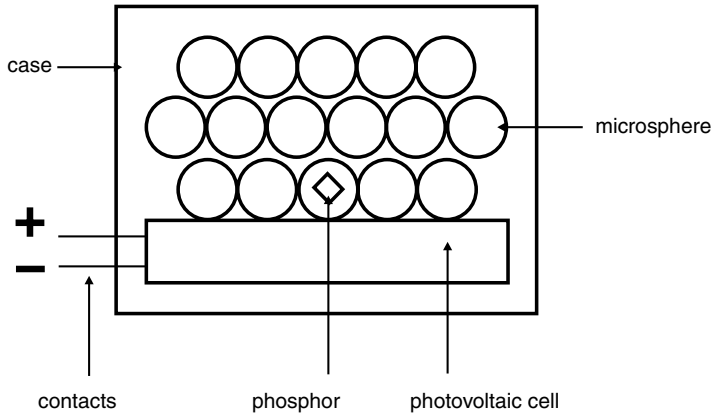


**Figure 1.4d** Self-luminous microspheres–containing light source–based battery. (From Rivenburg, R.C. et al., U.S. Patent 5,443,657, 1995.)

saturated with tritium at a pressure of 1 rather than 100 atm (as in the case above), is characterized by about 100 times less tritium and 50 to 100 times less radiosity.

At the same time, according to Renschler et al.,[29] radiosity of the light source decreases over 4 years proportionally to decreasing tritium activity. Apparently, with such light sources it will be possible to manufacture a battery with specific (per unit activity) electrical power, $Q$, of 0.5 μW/Ci. Although the specific power of this battery would be 100 times smaller than that of the light source with energy radiosity of 23 μW/cm$^2$, the fact that its specific power degrades only proportionally to the tritium decay makes such an option preferable.

The characteristics of actual models of batteries employing tritium gas–filled light sources are presented in Table 1.5 (item 10). The electric power of such batteries can be improved by no more than two- to threefold by optimizing the design and components employed, e.g., by utilizing converters (photovoltaics) with higher conversion efficiency, $\eta_{l\text{-}el}$. The batteries employing microsphere illuminators are relatively powerful and miniature. At the same time, lack of data on loading activity and long-term luminosity prevents unambiguous characterization of this device.

Table 1.5 suggests a relatively high efficiency of indirect conversion of radioactive decay energy to electricity compared to other conversion methods. The potential of indirect conversion will be unambiguously demonstrated only when better prototypes of the sort described are built and tested.

### 1.2.5 Light-Concentration Schemes for Indirect-Conversion Nuclear Batteries

In spite of the long history of the indirect conversion approach to nuclear batteries, some new designs have been proposed recently. Waveguide-based light concentration schemes look very promising and will be discussed. One of the major barriers to nuclear battery commercialization is self-absorption of the ionizing radiation in direct- and indirect-conversion schemes requiring large semiconductor

**Table 1.5 Parameters of Indirect-Conversion Betavoltaic Batteries**

| | Battery Units | | | Battery Parameters | | | | | |
|---|---|---|---|---|---|---|---|---|---|
| No. | Isotope | Light Source | Photovoltaic | $W$, Ci | $g_m$, μW | $v$, cm³ ($S$[a], cm²) | $Q$, μW /Ci | $\eta_{ind}$, % | Ref. |
| 1 | $^{147}$Pm | Luminophore based on CdS with $^{147}$Pm incorporated into the lattice | Silicon | 3.3 | 12 | — | 3.64 | 1 | 8 |
| 2 | $^{90}$Sr | Xenon containing a dust of radioactive material | Doped diamond, aluminum nitride | $6 \cdot 10^6$ | $10^{10}$ | $10^6$–$10^7$ | $1.7 \cdot 10^3$ | 25 | 11 |
| 3 | $^{208}$Po | | | $1.3 \cdot 10^6$ | | | $7.7 \cdot 10^3$ | 25 | |
| 4 | $^{228}$Ra | | | $3.5 \cdot 10^5$ | | | $2.8 \cdot 10^4$ | — | |
| 5 | $^{228}$Th | | | $2.2 \cdot 10^5$ | | | $4.5 \cdot 10^4$ | — | |
| 6 | $^{238}$U | | | $1.9 \cdot 10^5$ | | | $5.3 \cdot 10^4$ | — | |
| 7 | $^{238}$Pu | | | $1.2 \cdot 10^6$ | | | $8.3 \cdot 10^3$ | 25 | |
| 8 | $^{3}$H | Aerogel–phosphor (ZnS) composition saturated with tritium | $A^3B^5$ (GaAs, AlGaAs, GaAsP, GaP) | 3200 | 2000 | 32 | 0.625 | 1.8 | 30 |
| 9 | $^{3}$H | Aerogel–phosphor (ZnS) composition saturated with tritium | a-SiH | 5800 | 2000 | 60 | 0.345 | 1 | 30 |
| 10 | $^{3}$H | Gas-filled tritium light sources | AlGaAs | 0.5<br>1.2 | 0.09<br>0.15 | (3.4)<br>(3.4) | 0.18<br>0.12 | 0.5<br>0.4 | See Section 7.2.8 (Chap. 7) |
| 11 | $^{3}$H | Panel comprising microspheres 0.025 cm in diameter | AlGaAs | — | 50 | (7.5) | — | — | 28 |

[a] S is the photovoltaic converter area.

surfaces to collect tiny radiation flux. Since semiconductor cost dominates battery cost, the large semiconductor surface area increases the cost-to-power ratio. Direct conversion also has a central problem of semiconductor radiation damage, which suggests the value of indirect conversion designs in which the semiconductor is not exposed to highly ionizing radiation.

Use of light concentration schemes based on waveguides improves indirect design by increasing the intensity of light incident on the photovoltaic cell. This greatly improves the efficiency of the photovoltaic, which is essential for miniaturization and cost reduction. Multilayer structures needed for practical energy output are cheaper to fabricate when one of the repeating components, in this case the photovoltaic cell, is removed from the structure and placed outside. Such a design better protects the photovoltaic from radioisotope diffusion, which can radiolytically and chemically damage the semiconductor.

Use of waveguide-based light concentration is well known in the technology of solar cells.[31] Large-area flat waveguides luminesce under excitation by sun radiation. Concentrated light is emitted at the edge of the waveguide and coupled to the photovoltaic; the effect is to increase the light flux at the surface of the photovoltaic. The same idea may be used for a radioluminescent light source in which a waveguide luminesces under exposure to ionizing radiation.

#### *1.2.5.1 Nuclear Battery Design*

Figure 1.5 shows a nuclear battery design using waveguide principles.[32] Hermetic sealing of the radioisotope with a tritium getter such as 1,4-bis(phenylethynyl)benzene (DEB) prevents accidental isotope leakage. Scintillation glass waveguides are coated with thin metal mirrors (or a high difference refractive index barrier) and a radioisotope or its compound. Waveguides may be in the form of fibers or plates. The isotope or its compound generates beta radiation; the beta particles penetrate the scintillating waveguide to generate photons that are piped to the emitting edge. A radiation-hard borosilicate glass window is optically coupled between the waveguide and photovoltaic, preventing radioisotope diffusion to the semiconductor. The spectral response of the photovoltaic cell should be matched to emission of the scintillating material. The radioisotope may be advantageously incorporated into the waveguide; for example, promethium oxide may be incorporated into the glass.

Advantages of the nuclear battery using scintillating waveguides are:

- The semiconductor is not exposed to ionizing radiation.
- Photovoltaic cell conversion efficiency is increased by an increase of light flux.
- Smaller photovoltaic cells offer miniaturization and cost reductions.
- Waveguides may be fabricated in device-compatible shapes with thickness equal to the penetration depth of isotope betas, thereby allowing further miniaturization.
- Emission spectra of radioluminescent material can be tuned to better match spectral sensitivity of the photovoltaic cell, greatly increasing efficiency.
- There is a possibility of incorporating the isotope into the scintillating material to improve power density and efficiency.

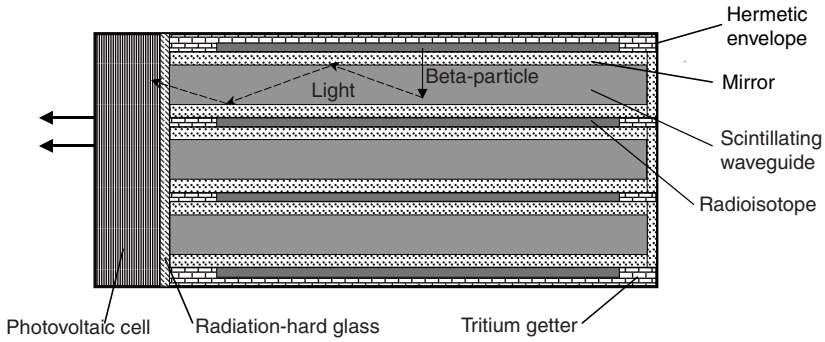


**Figure 1.5** Schematic view of the radioluminescent waveguide–based light concentration battery design.

Scintillation glass will work if the radioluminescent light is successfully piped to the emitting edge of the waveguide, which is possible when several conditions are fulfilled. Material for the waveguide should not absorb or scatter the radioluminescent light; this light must be reflected on the interface between waveguide and the surrounding media. The first option is to coat the waveguide with a metal mirror, which should have high reflectivity. The problem is that even a thin film of the metal will absorb part of the useful beta radiation. To minimize this effect, metal with low Z (atomic number) is needed. Aluminum meets both requirements. Another option is to put the waveguide having refraction coefficient $n_1$ into the surrounding media with lower refraction coefficient $n_2$. Then part of the radioluminescent light emitted at the angle lower than critical will undergo multiple total internal reflection and be piped to the edge. (See Figure 1.6.)

Light emitted within the solid angle $2\Phi$ escapes the waveguide and is therefore lost for useful utilization. The value of critical angle is defined as follows:

$$\Phi = \arcsin\left(n_2/n_1\right) \tag{1.24}$$

For example, if the waveguide is made of glass or plastic with $n_1 = 1.6$ and surrounded by gas with $n_2 = 1$, then $\Phi = 39^\circ$. Trapping efficiency, $\eta_{trap}$, is the efficiency of light transferred through the waveguide[31]:

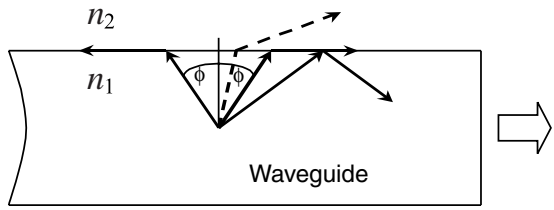


**Figure 1.6** Scheme of light propagation in the waveguide.

$$\eta_{trap} = \cos\Phi \tag{1.25}$$

In this example, $\eta_{trap} = 0.78$. If $n_1 = 1.7$, then $\eta_{trap} = 0.81$. Thus, about 80% of radioluminescent light may be trapped in the waveguide. Instead of use with gas as the surrounding media, waveguides may be coated with cladding with a very low $n_1$ value. For example, silica aerogel has a refraction index close to 1.[33]

When light reaches the edge of the waveguide, total internal reflection plays a negative role, preventing part of the light from escaping the waveguide and reaching the photovoltaic. For better output, the emitting edge must be optically coupled to the photovoltaic with optical grease or glue. Antireflection coatings may also be useful.

#### *1.2.5.2 Suitable Radioluminescent Materials*

Light concentration schemes require efficient scintillators. Among the most efficient radioluminescent materials known are $A_2B_6$-based phosphors. Hamil and co-authors[34] suggested use of ZnS radioluminescent phosphor waveguides in a form of thin sheets or long whiskers mounted in a sealed envelope filled with tritium gas. However, $A_2B_6$ compounds are not very transparent for the emitted light, and self-absorption is a problem preventing concentration since, in the waveguide, light must travel a significant distance. To overcome the problem of light self-absorption, waveguiding plates have been tried; these are made of glass or other transparent material on which vapor-deposited thin films of radioluminescent phosphor have been deposited.[35] The distance that light can pass is increased, since most of the distance to the voltaic is in the glass.

To further decrease absorption losses, phosphor with better transparency to its own light has been used: cerium and europium doped-calcium sulfide. Use of comparatively thick plates will limit miniaturization and concentration possibilities. Using tritium gas will not allow very high specific power unless elevated pressures are used, which is not safe or practical.

Another class of efficient radioluminescent materials is alkali halides such as NaI(Tl) and CsI(Tl). This class of materials possesses low light absorption. Designs of radioluminescent light sources have been based on polished CsI(Tl) planar waveguides.[36] The authors fabricated a "sandwich" of monocrystal plates $35 \times 60$ mm in size and 0.4 to 0.5 mm thick. Between them, $^{35}S$ was dispersed in polyvinylalcohol. However, fabrication of thin alkali halide waveguides by polishing is costly and time consuming. Since the waveguide thickness must be comparable to the penetration depth of betas (or alphas if alpha emitter is used), use of tritium would require micrometer layers. An additional disadvantage of alkali halides is that they are hygroscopic and would require moisture protection. It is possible to utilize plastic scintillators that are used in the detection of penetration radiation, but their radiation stability is poor.

Scintillating glass is nearly ideal as a waveguiding material for this application. Glasses have good optical properties and have been used in detection and visualization of penetration radiation. Li-containing glasses are used for the detection of